The Design and Realization of a New Normalization Algorithm in Electromagnetic Tomography

[1,3]Liu Li and [2]Zhanjun Wang
[1]College of Physics Science and Technology,
[2]Department of Computer and Math, Shenyang Normal University, Liaoning, 110034, China
[3]College of Information Science and Engineering, Northeastern University,
Liaoning, 110001, China

Abstract: In this study, we introduce the new sensitivity normalizations of electrical impedance and electrical capacitance tomography. Moreover, in electromagnetic tomography, we proposed the irrationality of linear normalization of sensitivity matrix, thence the new sensitivity normalization model was established based on the analytical formula. The formula of the new sensitivity normalization was given. The normalization effect of new model was compared with the original one. The new sensitivity normalization was applied to the image reconstruction and evaluated the image quality using the criterion correlation. It is conclusion that the new sensitivity normalization model is more close to the original trend and got higher reconstruction image quality.

Key words: Electromagnetic tomography, normalization, sensitivity

INTRODUCTION

Electrical Tomography (ET) techniques include Electrical Impedance Tomography (EIT) (Purvis *et al*., 1993), Electrical Capacitance Tomography (ECT) (Xie *et al*., 1992) and Electromagnetic Tomography (EMT) (Peyton *et al*., 1996). The aim in ET is to reconstruct the passive electrical properties, conductivity δ and permittivity ε of tissues. In order to be able to reconstruct an image, a mathematical model and sensitivity matrices have to be derived. The forward model is normally solved with the Finite Element Method (FEM) (Hansen and Regularization, 1994; Ni *et al*., 2004). Yang *et al*. (2002) studies the adaptive calibration of a capacitance tomography system for imaging water droplet distribution. Xiong *et al*. (1998) analyses the imaging wet gas separation process by capacitance tomography. Yang *et al*. (2002) have a research of the physical mechanism and detectability limits of electromagnetic tomography. Ma *et al*. (2006) studies the hardware and software design Electromagnetic induction Tomography (EMT) system for high contrast process applications. Scharfetter *et al*. (2008) analyses the hardware for quasi-single-shot multifrequency Magnetic Induction Tomography (MIT): the Graz Mk2 system. Vauhkonen *et al*. (2008) proposes the a measurement system and image reconstruction in magnetic induction tomography. PENG *et al*. (2004) studies the image reconstruction algorithms for electrical capacitance tomography: state of the art. Sensitivity matrices are generally normalized using different approaches. Normalization is a dimensionless means of

simplifying calculation, which can convert the absolute value of the physical system into relative value. There are many different variables in ET, for example, the detection voltage, the image gray and the sensitivity. Even with the same physical variables, there is also a relatively large gap between their key composition. Therefore, the problem of large numbers eating small numbers will appear, that is, we will ignore the variance of a small variable, but in favor of the large variance information. In order to equally treat each variable, to eliminate the impact of the value gap, the original data need to normalization preprocessing before using them. Common normalization methods include linear function, logarithmic function and arc tangent function conversion method. Image reconstruction is the inverse problem of the forward model, which is serious ill in ET. It is very sensitive to noise of detection value, that is, tiny perturbations will lead to medium conductivity or magnetic permeability distribution rapidly changing, so can not get a stable solution. The normalized measured value or sensitivity help reduce the impact of noise. In general, the measurements of adjacent electrode pairs are much larger than the relative electrode combination (usually tens or even hundreds of times). In order to eliminate the effect and reduce systematic errors in the measurement system, before being applied reconstruction algorithm, the measurements and sensitivities are in need to be normalized.

In this study, we introduce the new sensitivity normalizations of electrical impedance and electrical capacitance tomography. Moreover, the new sensitivity

Corresponding Author: Liu Li, College of Physics Science and Technology, Shenyang Normal University, Liaoning, 110034, China

normalization model is built on the basis of its analytical solution, which is more in line with the distribution trend of the original sensitivity than the traditional linear normalization model. From the reconstructed images with the new one and evaluating image quality with the correlation, we can conclude that reconstructed images with new sensitivity normalization model has smaller imaging error and higher correlation than linear sensitivity normalization.

METHODOLOGY

Sensitivity normalization in electrical tomography: From the mathematical models of ET techniques can be seen, the measured value and sensitivity of the model are more complex. They are difficult to be solved by analytical methods, while analyzed by numerical methods commonly. Therefore, the above normalization models can not preprocess raw data, but need derive the specific normalization model according to mathematical models. For ECT, the measurement value and the sensitivity normalization model are based on the application process occasions and two-phase flow models (Yang *et al.*, 2004). The comparison of the relationships between the measured capacitance and the normalized capacitance for different distribution models (parallel, series and Maxwell) was presented in study (Yang *et al.*, 2002). For different types of multi-phase flow model, you can use different normalization model, even with the same image reconstruction algorithms, image quality can vary considerably. Yang studies these models and points out that the series model in most of the flow distribution can improve the quality of image reconstruction. It is more suitable for serious non-linear phase holdup or the equivalent dielectric constant (Yang *et al.*, 2004). ERT usually uses logarithmic sensitivity normalized form.

EMT is able to distinguish two different dielectric constant or magnetic permeability medium. The forward problem of EMT is aimed at studying the magnetic vector changes of the detection coil sensor and inverse problem is reconstructing magnetic permeability distribution, i.e., exploiting the magnetic vector potential to reconstruct image. The EMT system mainly reconstructs the object field for the different permeability of two-phase flow or multi-phase flow. In order to improve the quality of the reconstruction image, the measurement of the magnetic vector potential and the sensitivity matrix should be normalized. The traditional normalization methods are under the premise that the EMT system mathematical model is linear. Normalized magnetic vector potential satisfies the linear normalization function:

$$\lambda_{old} = \frac{A_m - A_l}{A_h - A_L} \tag{1}$$

where λ_{old} is normalized magnetic vector potential between a pair of coils and A_m, A_h and A_L are the actual measured value, the full field measured value and the

empty field measured value between the same coils. From Eq. (1) can see, when the object field is full of low-permeability medium, the magnetic vector should be zero, when is full of high-permeability medium, the magnetic vector is equal to 1. When placing high-permeability medium into low-permeability medium, normalization magnetic vector potential is the linear interpolation between A_h and A_L.

However, object field is very complex and the relationship between the distribution of magnetic permeability and magnetic vector satisfies:

$$\nabla^2 \vec{A} - jw\mu\vec{A} = 0 \tag{2}$$

Therefore, linear normalization formula can not be applied to EMT. In order to get the normalized formula of the magnetic vector potential and sensitivity, we must deduce the relationship between them from analytical solution of Eq. (2).

Derivation of the new normalization model in EMT: For two-dimensional space, $\vec{A}$ only has vertical component, so Eq. (2) can be simplified to scalar equations, i.e.,

$$\nabla^2 A_1 - k^2 A_1 = 0 \tag{3}$$

$$\nabla^2 A_2 = 0 \tag{4}$$

where A_1 and A_2 are magnetic vector potential within imaged objects or in the medium and $k = \sqrt{jw\delta_1\mu_1}$. In the polar coordinate system (r, φ), which looks the centre of the imaged objects as the origin, Eq. (3) and (4) can convert tol:

$$\frac{1}{r}\frac{\partial}{\partial r} r \frac{\partial A_1}{\partial r} + \frac{1}{r^2}\frac{\partial^2 A_1}{\partial \varphi^2} - kA_1 = 0 \tag{5}$$

$$\frac{1}{r}\frac{\partial}{\partial r} r \frac{\partial A_2}{\partial r} + \frac{1}{r^2}\frac{\partial^2 A_2}{\partial \varphi^2} = 0 \tag{6}$$

Solving the Eq. (2) by separate variable method and supposing $A_1(r, \varphi), = R(r) \Phi(\varphi)$, Eq. (5) can simplify to two differential equations, i.e.,

$$\Phi'' + v^2\Phi = 0 \tag{7}$$

$$r^2 R'' + rR' - (k^2 - v^2)R = 0 \tag{8}$$

The general solution of Eq. (7) is:

$$\Phi = E \cos (n\varphi) + F \sin (n\varphi) \tag{9}$$

Equation (8) is Bessel Function for virtual argument and its solution is:

$$R_v(kr) = AK_v(kr) + BK_{-v}(kr) \qquad (10)$$

where, $K_v(kr) = \dfrac{\pi}{2\sin v\pi}[I_{-v}(kr) - I_v(kr)]$ and $K_v(kr)$ and I_v (kr) are arguments of the first type and the second type of Bessel Function. Therefore, the general solution of Eq. (5) is:

$$A_1(r,\varphi) = \sum_{n=1}^{\infty}[E\cos(n\varphi) + F\sin(n\varphi)I$$
$$[AK_n(kr) + BK_{-n}(kr)] \qquad (11)$$

In the same way, the general solution of Eq. (6) is:

$$A_2(r,\varphi) = \sum_{n=1}^{\infty}[Cr^n + Dr^{-n}]$$
$$[P\cos(n\varphi) + Q\sin(n\varphi)] \qquad (12)$$

The boundary conditions of EMT system include: On the boundary surface of the object and medium, A is continuous, i.e.,

$$A_1(a, \phi) = A_2(a, \phi)$$

- On the boundary surface of the object and medium, the tangential component H is continuous too, i.e.,

$$\left.\frac{1}{\mu_1}\frac{\partial A_1}{\partial r}\right|_{r=a} = \left.\frac{1}{\mu}\frac{\partial A_2}{\partial r}\right|_{r=a}$$

- On the boundary of the object field, satisfy:

$$\left.\frac{\partial A_2}{\partial r'}\right|_{r'=R} = \mu_2 K\sin\varphi$$

where the centre of the objet field is the origin of the polar coordinate system $(r'\varphi')$.

When the measured object is located in the centre of the object field, the magnetic vector potential A_1 and A_2 are deduced by Xiong Hanliang in study (Xiong *et al.*, 1998):

$$A_1(r,\varphi) = \frac{4\mu_1\mu_2 K}{kQ}I_1(kr)\sin\varphi \qquad (13)$$

$$A_2 = \mu_2 KP(r + \frac{a^2}{r}T)\sin\varphi \qquad (14)$$

where,

$$T = \frac{(\mu_1 - \mu_2)I_0(ka) - (\mu_1 + \mu_2)I_2(ka)}{(\mu_1 + \mu_2)I_0(ka) - (\mu_1 - \mu_2)I_2(ka)}$$

$$P = \frac{1}{1 - a^2 gT}$$

$$Q = [(\mu_1 + \mu_2) - (\mu_1 - \mu_2)a^2 g]I_0(ka) -$$
$$[(\mu_1 - \mu_2) - (\mu_1 + \mu_2)a^2 g]I_2(ka)$$

$$g = \frac{\rho\sin\Phi - r_0\sin(2\Phi - \varphi_0)}{\rho^2(\rho\sin\Phi - r_0\sin\varphi_0)}$$

$$\rho = r_0\cos(\Phi - \varphi_0) + \sqrt{R^2 - r_0^2\sin^2(\Phi - \varphi_0)}$$

For the empty field, i.e., there is only low-permeability medium μ_2 in the object field and the magnetic vector potential is:

$$A_1 = \mu_2 = KR\sin\phi \qquad (15)$$

when there is only high-permeability medium μ_1 in the object field, i.e., for full field, the following formulas were established:

$$r_0 = 0; \rho = R; g = \frac{1}{R^2}; P = \frac{1}{1-T},$$

therefore:

$$A_h = \mu_2 KR\sin\varphi.\frac{1+T}{1-T} = A_l\frac{1+T}{1-T} \qquad (16)$$

when an object of permeability of μ_1 locates into the object field of low-permeability medium μ_2, the measured magnetic vector potential is:

$$A_2 = \mu_2 K\frac{R}{1 - \frac{a^2}{R^2}T}\left(1 + \frac{a^2}{R^2}T\right)\sin\varphi$$

$$= \mu_2 KR\sin\varphi\frac{R^2 + a^2 T}{R^2 - a^2 T}$$

$$= A_l\frac{R^2 + a^2 T}{R^2 - a^2 T} \qquad (17)$$

$$= A_l\frac{(R^2 + a^2)A_h + (R^2 - a^2)A_l}{(R^2 - a^2)A_h + (R^2 + a^2)A_l}$$

Suppose $a = \lambda R$, where λ is normalization parameter, therefore:

$$\frac{A_2}{A_l} = \frac{(1 + \lambda^2)A_h + (1 - \lambda^2)A_l}{(1 - \lambda^2)A_h + (1 + \lambda^2)A_l}$$

$$\lambda = \sqrt{\frac{(A_h + A_l)(A_2 - A_l)}{(A_h - A_l)(A_2 + A_l)}} \qquad (18)$$

This shows that the EMT sensitivity normalization is not linear and the normalized parameter is related with the magnetic vector of the full field and empty field. The traditional sensitivity normalization adds a new factor to the new model:

$$\lambda = \sqrt{\lambda_{old} \frac{A_h + A_l}{A_2 + A_l}} \qquad (19)$$

Suppose , $k = \dfrac{A_h + A_l}{A_2 + A_l}$ Eq. (19) can convert to:

$$\lambda = \sqrt{k\lambda_{old}} \qquad (20)$$

where k is correction parameter.

SIMULATION AND RESULTS

For 8 coils EMT system, each coil in turn do the excitation and the remaining coils do detection. Finite Element Method (FEM) (Ma *et al.*, 2006) to solve forward problem analyzes the measurement and establish the sensitivity matrix. Use two normalization methods to preprocess the sensitivity matrix. According to Eq. (1) and (20), we obtain the normalized approach known as he original normalization method and he new normalization method Figure 1 displays the centre and the edge of sensitivity distribution using original and new sensitivity normalization methods. For 70 triangulation units at the centre of the object field, normalized sensitivity distribution is shown in Fig. 1a and normalization sensitivity of near edge of the object field is shown in Fig. 1b, in which the horizontal axis indicates split unit number and the vertical axis represents normalized value, where blue circles display the new method and red circles display the original normalization sensitivity method. As can be seen from two kinds of normalization results:

- For the data variation, sensitivity of new normalization algorithm and linear normalization is similar, but more concentrated, which is corresponding to the actual sensitivity of the distribution.
- The sensitivity of the centre with higher concentration, concentrated between 0.3 and 0.8, so the new model can improve the relevance of the reconstructed image.

Four flow prototypes are reconstructed by standard Tikhonov regularization (Scharfetter *et al.*, 2008) and
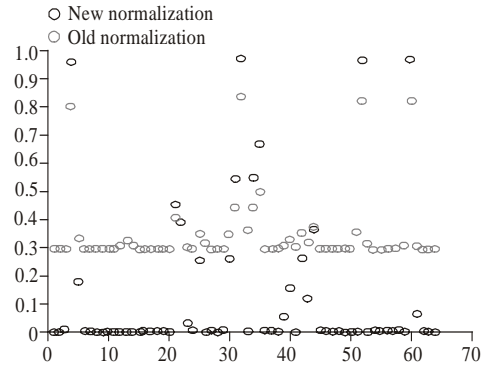
(a) Normalization sensitivity of the centre of the object field
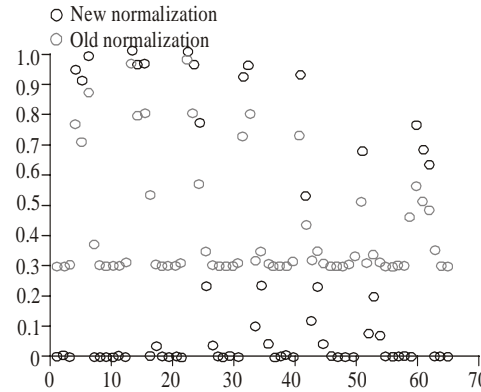
(b) normalization sensitivity of the edge of the object field

Fig. 1: Normalization sensitivity using original and new normalization methods

Table 1: Correlation for orginial normalization sensitivity & new normalization sensitivity

	(a)		(b)		(c)		(d)	
	ON	NN	ON	NN	ON	NN	ON	NN
Landweber	0.80	0.81	0.66	0.80	0.61	0.72	0.64	0.69
Tikhonov	0.86	0.88	0.75	0.82	0.69	0.74	0.71	0.73

ON: old normalization; NN: new normalization

Landweber iteration methods (Vauhkonen *et al.*, 2008) in Fig. 2. Correlation coefficient (Peng *et al.*, 2004) reflects the image gray correlation between the original and the reconstructed images, which lists in Table 1. In order to compare four normalization model of image quality, image gray doesn execute threshold filter.

It can be seen from the image reconstruction and image evaluation that the new sensitivity normalization algorithm for overcoming imaging error is more effective than the original algorithm, i.e., the correlation is relatively high, especially to improve the sensitivity of the centre object field. So imaging error for centre flow, shown in Fig. 2b, is greatly reduced and is closer to the original image than original sensitivity normalization.
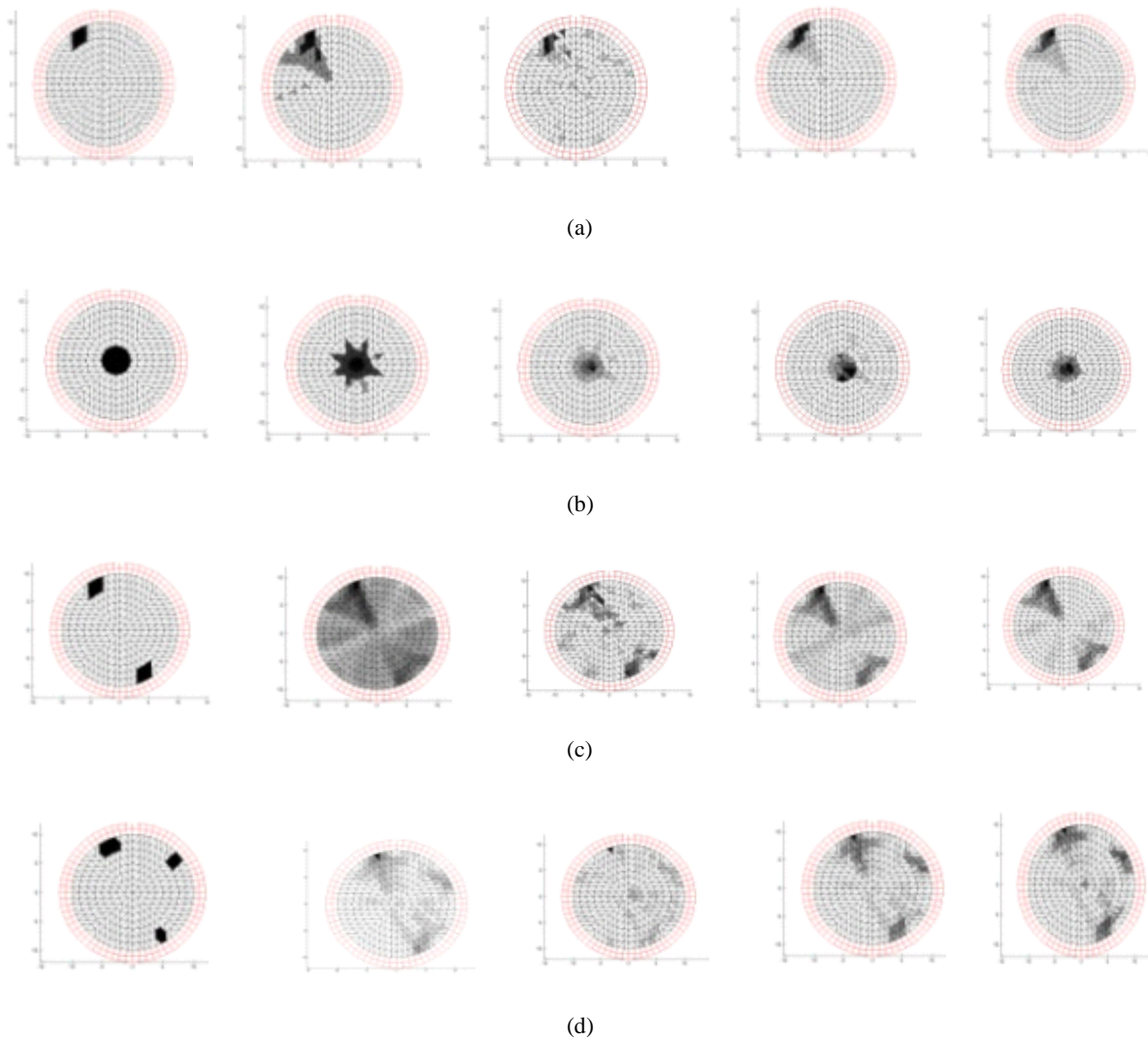
(a)

(b)

(c)

(d)

Fig. 2: Image reconstruction for 4 models used landweber iteration, tikhonov regularization algorithms with new normalization and original normalization sensitivities

CONCLUSION

The new sensitivity normalization model is built on the basis of its analytical solution, which is more in line with the distribution trend of the original sensitivity than the traditional linear normalization model. From the reconstructed images with the new one and evaluating image quality with the correlation, we can conclude that reconstructed images with new sensitivity normalization model has smaller imaging error and higher correlation than linear sensitivity normalization.

ACKNOWLEDGMENT

REFERENCES

Hansen, P.C., 1994. Regularization Tools: A Matlab Package for Analysis and solution of Discrete Ill-posed Problems. Numerical Algorithms, pp: 1-35.

Ma, X., A. Peyton, S.R. Higson, A. Lyons and S.J. Dickinson, 2006. Hardware and software design Electromagnetic Induction Tomography (EMT) system for high contrast process applications. Meas. Sci. Technol, 17: 111-119.

Ni, G. and S. Yang, *et al*., 2004. Engineering Computational Electromagnetics. Mechanical Industry Press.

Peng, L., H. Lug and W.Q. Yang, 2004. Image reconstruction algorithms for electrical capacitance tomography: State of the art. J. Tsinghan Univ. Sci. Tech., 44(4): 478-484.

Peyton, A.J., Z.Z. Yu, G. Lyon, S. Al-Zeibak, J. Ferreira, J. Velez, F. Linhares, A.R. Borger, H.L. Xiong, N.H. Saundevs and M.S. Beck, 1996. An overview of electromagnetic inductance tomography: Description of three different systems. Meas. Sci. Technol., 7(3): 261-271.

Purvis, K.R., R.C. Tozer, D.K. Anderson and I.L. Freeston, 1993. Induced current impedance tomography. IEEE Proc. pt. A, 140(2): 135-141.

Scharfetter, H., A. Kostinger and S. Issa, 2008. Hardware for quasi-single-shot multifrequency Magnetic Induction Tomography (MIT): The Graz Mk2 system. Physiol. Meas., 29: 431-443.

Vauhkonen, M., M. Hamsch and C.H. Igney, 2008. A measurement system and image reconstruction in magnetic induction tomography. Physiol. Meas., 29: 445-454.

Xie, C.G., S.M. Huang, B.S. Hoyle, R. Thorn, C. Lenn, D. Snowden, M.S. Beck, 1992. Electrical capacitance tomography for flow imaging: System model for development of image reconstruction algorithms and design of primary sensors. IEEE Proc. G, pp: 89-98.

Xiong, H., Y. Dong and A. Wang, 1998. Physical mechanism and detectability limits of electromagnetic tomography. J. Tianjin Univ., 31(2): 136-142.

Yang, W.Q., T. Nguyen, M. Betting, A. Chondronasios and S. Okimoto, 2002. Imaging wet gas separation process by capacitance tomography. IS&T/SPIE 14 Symposium, pp: 347-358.

Yang, W.Q., A. Chondronasios and S. Nattrass, V.T. Nguyen, M. Betting, I. Ismail and H. McCann, 2004. Adaptive calibration of a capacitance tomography system for imaging water droplet distribution. Flow Meas. Instrum., 15: 249-258.